Gyrokinetic Studies of Turbulence in Steep Gradient Region: Role of Turbulence Spreading and $\mathbf{E} \times \mathbf{B}$ Shear

T.S. Hahm 1), Z. Lin 2), P.H. Diamond 3), G. Rewoldt 1), W.X. Wang 1), S. Ethier 1), O. Gurcan 3), W.W. Lee 1), J.L.V. Lewandowski 1), and W.M. Tang 1)

1) Princeton Plasma Physics Laboratory, P.O.Box 451, Princeton, NJ 08543, USA

2) University of California Irvine, Irvine, CA 92697, USA

3) University of California San Diego, La Jolla, CA 92093, USA

e-mail contact of main author: tshahm@pppl.gov

Abstract. An integrated program of gyrokinetic particle simulation and theory has been developed to investigate several outstanding issues in both turbulence and neoclassical physics. Gyrokinetic particle simulations of toroidal ion temperature gradient (ITG) turbulence spreading using the GTC code and its related dynamical model have been extended to the case with radially increasing ion temperature gradient, to study the inward spreading of edge turbulence toward the core. Due to turbulence spreading from the edge, the turbulence intensity in the core region is significantly enhanced over the value obtained from simulations of the core region only. Even when the core gradient is within the Dimits shift regime (*i.e.*, self-generated zonal flows reduce the transport to a negligible value), a significant level of turbulence and transport is observed in the core due to spreading from the edge. The scaling of the turbulent front propagation speed is closer to the prediction from our nonlinear diffusion model than one based on linear toroidal coupling. A calculation of ion poloidal rotation in the presence of sharp density and toroidal angular rotation frequency gradients from the GTC-Neo particle simulation code shows that the results are significantly different from the conventional neoclassical theory predictions. An energy conserving set of a fully electromagnetic nonlinear gyrokinetic Vlasov equation and Maxwell's equations, which is applicable to edge turbulence, is being derived via the phase-space action variational Lie perturbation method. Our generalized ordering takes the ion poloidal gyroradius to be on the order of the radial electric field gradient length.

1. Introduction

Despite significant progress in experiment, theory and computation in recent years, the predictive capability of turbulence and transport in magnetically confined plasmas is limited to case-by-case direct numerical simulations of better understood systems. Serious challenges remain due to the fact that virtually all models of fluctuation levels and turbulent transport are built on an assumption of *local balance* of linear growth with linear damping and nonlinear coupling to dissipation, *i.e.*, the traditional "local balance" paradigm of Kadomtsev et al[1]. Such models thus necessarily exclude mesoscale dynamics, which refers to dynamics on scales larger than a mode or integral scale eddy size, but smaller than the system. In particular, transport barriers, avalanches, heat and particle pulses are all mesoscale phenomena[2, 3, 4, 5]. Such mesoscale phenomena necessarily introduce an element of nonlocal interaction, which is strongly suggested by experiments, but absent from the models.

In our previous studies[6, 7], we have identified and studied in depth the simplest nontrivial problem of turbulence spreading corresponding to the spatio-temporal propagation of a patch of turbulence from a region where it is locally excited to a region of weaker excitation, or even of local damping. Our results highlighting the importance of growth and damping rate profiles in the spatio-temporal evolution of turbulence were in broad, semi-quantitative agreement with global gyrokinetic simulations of core ITG turbulence[7]. In particular, it has been demonstrated that turbulence spreading into the linearly stable zone can cause deviation of the transport scaling from the gyroBohm scaling which is expected from local characteristics of turbulence. From these observations, it is clear that turbulence spreading plays a crucial role in determining turbulence and transport profiles in the core-edge connection region where the gradient increases rapidly as a function of radius.

Turbulence propagation and overshoot vitiate the conventional picture of turbulent transport based upon a local balance, which is assumed in virtually all modeling codes. Moreover, energy propagation from the strongly turbulent edge into the core can effectively renormalize the edge "boundary condition" used in the modelling calculation. This ultimately feeds into predictions of pedestal extent.

2. Gyrokinetic Simulation of Turbulence Spreading from Edge

In this paper, we focus our studies on the case with radially increasing ion temperature gradient to study the inward spreading of edge turbulence toward the core. We note that the possibility of edge turbulence influencing core turbulence has been discussed before[8, 9]. Our main computational tool is a well benchmarked, massively parallel, full torus gyrokinetic toroidal code (GTC) [10]. Toroidal geometry is treated rigorously, *e.g.*, the radial variations of safety factor q, magnetic shear $\hat{s}$, and trapped particle fraction are retained in global simulations. Both linear and nonlinear wave-particle resonances, and finite Larmor radius effects are treated in gyrokinetic particle simulations [11]. The GTC code employs magnetic coordinates which provide the most general coordinate system for any magnetic configuration possessing nested surfaces. The global field-aligned mesh provides the highest possible computational efficiency without any simplification in terms of physics models or simulation geometry. Unlike other quasi-local codes in flux-tube geometry which remove important radial variations of key equilibrium quantities, such as safety factor, magnetic shear, and temperature gradient, and use periodic boundary conditions in the radial direction, GTC does not rely on the ballooning mode formalism which becomes dubious in describing meso-scale phenomena including turbulence spreading.

All simulations reported in this paper use representative parameters of tokamak plasmas [12] with the following local parameters: $R_0/L_n = 2.2$, $q = 1.4$, $\hat{s} \equiv (r/q)(dq/dr) = 0.78$, $T_e/T_i = 1$, and $a/R_0 = 0.36$. Here R_0 is the major radius, a is the minor radius, L_T and L_n are the ion temperature and density gradient scale lengths, respectively, T_i and T_e are the ion and electron temperatures, and q is the safety factor. Our global simulations use fixed boundary conditions with electrostatic potential $\delta\phi = 0$ enforced at $r < 0.1a$ and $r > 0.9a$. Simplified physics models include: a parabolic profile of $q = 0.854 + 2.184(r/a)^2$. The temperature gradient profile mainly consists of two regions, a "core region" from $r/a = 0.2$ to 0.5, and an "edge region" from $r/a = 0.5$ to 0.8 and a gradual decrease to much smaller values towards $r/a = 0.1$ and $r/a = 0.9$. A circular cross section, and electrostatic fluctuations with adiabatic electron response, are used in the simulations discussed in this paper.

The ion temperature gradient value in the core is based on our previous studies. In the first case summarized in Fig. 1, $R/L_{Ti} = 6.9$ in the core, which is above the effective critical gradient in the presence of zonal flows $R/L_{crit} = 6.0$, while in the second case summarized in Fig. 2, $R/L_{Ti} = 5.3$ is within the Dimits shift regime[12]. We double the value of the ion temperature gradient at the edge to model the stronger gradient at the tokamak edge. We have adopted this two step feature for the ion temperature gradient to make comparisons with our previous core simulations[13, 7] and an analytic model[14] feasible.

Fig. 1 shows the spatio-temporal evolution of the ITG turbulence envelope for the first case with $R/L_{Ti} = 6.9$ in the core. The simulation was run until $t = 300L_{Ti}/c_s$ when the turbulence apparently ceases to spread further. The initial growth in the edge region with $R/L_{Ti} = 13.8$ and a higher linear growth rate is apparent from Figs. 1(a),1(b). By the time the edge turbulence saturates at $t \sim 200L_{Ti}/c_s$, turbulence spreading towards the core is already well in progress. The turbulence spreading can be characterized by nearly ballistic ($\sim t$) propagation of the front with a velocity $U_x \simeq 2.5(\rho_i/R)c_s$. The time average value of fluctuation intensity during the last 1/3 of simulation duration at $r = 0.4a$ (core) is $I \sim 36.5(\rho_i/a)^2$, which is about 60 percent above the value $I \sim 22.0(\rho_i/a)^2$ from the core simulation with a maximum gradient $R/L_T = 6.9$[7].

Fig. 2 shows the spatio-temporal evolution of ITG turbulence envelope for the second case with $R/L_{Ti} = 5.3$ in the core. The simulation was run until $t = 500L_{Ti}/c_s$ when the turbulence apparently ceases to spread further. The initial growth in the edge region with $R/L_{Ti} = 10.6$ and a higher linear growth rate is apparent from Figs. 2(a), 2(b). By the time the edge turbulence saturates at $t \sim 300L_{Ti}/c_s$, turbulence spreading towards the core is already well under way although the core region is effectively stable (i.e., within the Dimits shift regime) due to self-generated zonal flows. The turbulence spreading is better characterized by an exponential decay in space (with a characteristic skin depth $\sim 25\rho_i$ as we reported before in the context of core simulations[6, 7]), rather than by the propagation of a front. The time average value of the fluctuation intensity during the last 1/3 of the simulation duration at $r = 0.4a$ (core) is $I \sim 12.7(\rho_i/a)^2$, while the core simulation with a maximum gradient $R/L_T = 5.3$ would have yielded a near zero value in the absence of collisional damping of zonal flows[13].

We have also performed a GTC nonlinear simulation for $R/L_T = 9.0$ in the core, and $R/L_T = 18.0$ in the edge. The results are qualitatively similar to the case in Fig. 1 with $R/L_{Ti} = 6.9$ in the core. The front propagation velocity was $U_x \simeq 4.4(\rho_i/R)c_s$. The time average value of the fluctuation intensity during the last 1/3 of the simulation duration at $r = 0.4a$ (core) was $I \sim 65.1(\rho_i/a)^2$.

3. Analytic Theory of Turbulence Spreading from Edge

Our analytic study of turbulence spreading is based on an equation for the local turbulence intensity $I(x,t)$, which includes the effects of local linear growth and damping, spatially local nonlinear coupling to dissipation and spatial scattering of turbulence energy induced by nonlinear coupling[6, 14, 15].

$$\frac{\partial I}{\partial t} = \frac{\partial}{\partial x}\chi(I)\frac{\partial I}{\partial x} + \gamma(x)I - \alpha I^{1+\beta} \tag{1}$$

The terms on the RHS correspond to nonlinear spatial scattering (*i.e.*, typically $\chi(I) \sim \chi_0 I^\beta$ where $\beta = 1$ for weak turbulence, and $\beta = 1/2$ for strong turbulence), linear growth and damping, and local nonlinear decay, respectively. Here α is a nonlinear coupling coefficient. Note that α and χ_0 could be functions of radius. This equation is the irreducible minimum of the model, to which additional equations for other fields, and contributions to dynamics which feed back on I, may be added. To pursue a study of turbulence spreading based on linear eigenmodes in toroidal geometry, one should consider a higher order ballooning mode formalism[16]. Note that the above equation manifests the crucial effect of spatial coupling in the nonlinear diffusion term. This implies that the integrated fluctuation intensity in a region of extent $\triangle$ about a point x (i.e. $\int_{x-\triangle}^{x+\triangle} I(x')dx'$) can grow, *even for negative* $\gamma(x)$, so long as $\chi(I)\partial I/\partial x|_{x-\triangle}^{x+\triangle}$ is *sufficiently large.* Alternatively, I can decrease, *even for positive* $\gamma(x)$, should $\chi(I)\partial I/\partial x|_{x-\triangle}^{x+\triangle}$ be *sufficiently negative.* Thus, the *profile* of fluctuation intensity is crucial to its spatio-temporal evolution. These simple observations nicely illustrate the failure of the conventional local saturation paradigm[1], and strongly support the argument that propagation of turbulence is a crucial, fundamental problem in understanding confinement scalings for fusion devices in which growth and damping rate profiles vary rapidly in space. Focusing on the weak turbulence regime in which global gyrokinetic simulation results are well documented[13], we take $\beta = 1$ for the rest of this paper.

We can make further analytic progress for profiles of $\gamma(x)$, α, and χ_0 which are constant in radius. Equation (1) is obviously a variant of the well-known Fisher-KPP equation for logistic-limited epidemic propagation[17, 18] with nonlinear diffusion. It is well-known that a reaction-diffusion type equation including the Fisher-KPP equation exhibits a *ballistic* propagating front solution. Both analytic and numerical solutions have been presented in detail in Ref [14]. The front velocity is simply given by $U_x = \sqrt{\gamma^2\chi_0/2\alpha}$. This solution indicates that the dynamics of $I(x,t)$ developing from a localized source of turbulence evolves in two steps. First, there is rapid growth to local saturation at $I = \gamma(x)/\alpha$. Second, the value $I = \gamma(x)/\alpha$ defines an effective value of the intensity dependent fluctuation diffusion $\chi = \chi_0 I = \chi_0\gamma/\alpha$. A classic Fisher-KPP front with velocity $U_x = \sqrt{\gamma\chi/2}$ is a consequence of the spatial coupling induced by a combination of local turbulence growth (with rate γ) and the effective diffusion ($\chi = \chi_0\gamma/\alpha$). It is crucial to note that the front of the turbulence intensity can propagate ballistically (*i.e.*, $x_{front} = U_x t$), even in the absence of toroidicity-induced coupling of neighboring poloidal harmonics. Therefore, the rapid propagation observed in simulations does not imply the dominance of linear coupling of poloidal harmonics. It should be considered as a more general nonlinear consequence of the dynamics. Since the scaling of U_x from our nonlinear theory (which increases with I and γ) is drastically different from the expectation from one due to linear toroidal coupling[9], our gyrokinetic simulations with the R/L_{Ti} scan provide crucial information on the dominant mechanism responsible for turbulence spreading. Since the front propagation velocity changed significantly from $U_x \simeq 2.5\rho_i c_s/R$ to $U_x \simeq 4.4\rho_i c_s/R$ as we increased the core gradient from $R/L_{Ti} = 6.9$ to $R/L_{Ti} = 9.0$, our gyrokinetic simulation results (which approximately scale like $U_x \propto (R/L_{Ti})^{1.5}$) agree better with the scaling from a nonlinear diffusion model[14] than with that from the linear toroidal couping $U_x \propto \rho_i c_s/R$. We also note that a numerical solution of Eq. (1) using the parameters in the simulations (a case with $R/L_{Ti} = 6.9$ at the core) shows a spatio-temporal evolution of turbulence patches (Fig. 3) which is very similar to the simulation results shown in Fig. 1.

In the first significant numerical study addressing turbulence spreading which has been performed in the context of a global mode couping analysis of toroidal drift waves[9], it was observed that the linear toroidal coupling of different poloidal harmonics played a dominant role in the convective propagation of fluctuations into a region with a zero level background of fluctuations in most parameter regimes. It is worthwhile to note that Ref. [9] was published before the important role of the self-generated zonal flows in regulating turbulence in toroidal geometry was fully realized[10]. In a similar fashion to the mean $\mathbf{E} \times \mathbf{B}$ flow shear causing decorrelation of turbulence in the radial direction[19, 20], the random shearing by zonal flows[21, 22] which has not been included in Ref.[9], would make the linear toroidal coupling much weaker. This is shown by the measured reduction in the radial correlation length of fluctuations[21] as radially global toroidal eigenmodes get destroyed by the zonal flows in gyrokinetic simulations[10]. Thus, we believe that the ballistic front propagation observed in our gyrokinetic simulations should be considered as a more general nonlinear consequence of the dynamics rather than as one due to linear toroidal coupling. We note that turbulence spreading has been observed in the absence of toroidal coupling as well[23, 24]. Analytic studies of turbulence spreading have been recently extended to subcritical turbulence as well[25].

The time-honored local saturation paradigm ($i.e.$, $\gamma/k_\perp^2 = D$) is clearly inadequate and incomplete. A finite initial pulse of turbulence spreads on dynamically interesting time scales, and more rapidly than rates predicted by considerations of transport, alone. For example, the predicted intensity velocity is the geometric mean of the local growth rate and the turbulent diffusivity. Efforts at modeling based on the local saturation paradigm should be reconsidered. Since turbulence can tunnel into marginal or stable regions, fluctation energy originating at the strongly turbulent edge may spread into the marginal core relatively easily, thus producing an intermediate region of strong turbulence. This phenomenon blurs the traditionally assumed distinction between the "core" and "edge", and suggests that the boundary between the two is particularly obsture in L-mode. It also identifies one element of the global profile readjustment which follow the L→H transition, namely the quenching of turbulence in the core which originated at the edge.

4. Simulation of Neoclassical Physics in Steep Gradient Region

In assessing the confinement properties of toroidal plasmas, it is important to accurately calculate the neoclassical dynamics, which set the minimum level of transport in such systems. There remain in present tokamak experiments significant unresolved neoclassical issues associated with steep pressure gradients, large rotation with strong shear, *etc.* Another important issue which is missing in theories is the self-consistent electric field which is established to maintain ambipolar transport. This equilibrium electric field may change neoclassical transport by changing the particle orbits[26]. The sheared equilibrium electric field is also believed to play an important role in determining the turbulence level. When these effects are properly taken into account, it is obviously of interest to revise the neoclassical physics in realistic toroidal plasmas.

We have developed a generalized global particle-in-cell (PIC) code, GTC-Neo[27], which employs the δf method to solve the drift kinetic equation together with the Poisson equation governing the ambipolar electric field in generalized toroidal geometry, for studying neoclassical physics and equilibrium electric field dynamics. The main physical and numerical features of GTC-Neo include self-consistent ambipolar electric field dynamics, fully global geometry effects, finite orbit effects (nonlocal transport), and systematic treatment of plasma rotation. Two species, main ions and electrons, are simulated at present, and extension to include impurities and energetic particles is ongoing.

The general geometry capability allows us to assess collisional heat, particle and angular momentum flux, the equilibrium radial electric field, bootstrap current and poloidal flow velocity, *etc.*, of a real machine for experimental comparison, directly using the measured plasma profiles and the corresponding MHD equilibrium.

We have applied this new capability to study the finite orbit physics of neoclassical transport and the radial electric field dynamics in shaped plasmas, including NSTX, DIII-D, and JET. Interesting new results include the nonlocal and nondiffusive properties of ion thermal transport near the magnetic axis, and the modifications of bootstrap current, radial electric field and ion poloidal flow velocity with large pressure gradient and/or large toroidal rotation with strong shear. A result for ion poloidal flow in a toroidally rotating plasma is presented in Fig. 4. It shows that strong sheared toroidal rotation (in the region $0.3 < r/a < 0.7$), in addition to the well known temperature gradient term, can drive a significant poloidal flow. It is suggested that direct measurement of poloidal flow is required to test the theory.

5. Extensions of Nonlinear Gyrokinetic Formalism to Edge

An energy conserving set of a fully electromagnetic nonlinear gyrokinetic Vlasov equation and Maxwell's equations, which is applicable to both L-mode turbulence with large amplitude and H-mode turbulence in the presence of high $\mathbf{E} \times \mathbf{B}$ shear, is being derived via the phase-space action variational Lie perturbation method which ensures the preservation of the conservation laws of the underlying Vlasov-Maxwell system. Conservation of energy and phase-space volume becomes more important as long term gyrokinetic simulations, well beyond the nonlinear saturation phase, become feasible with recent advances in computational power[7].

Our generalized ordering takes $\rho_{i\theta} \sim L_E \sim L_p$, as observed in the H-mode edge, with L_E and L_p being the radial electric field and pressure gradient lengths. We take $k_\perp \rho_i \sim 1$ for generality, and $e\delta\phi/T_i \sim \delta B/B \sim \rho_i/L_P < 1$ for finite fluctuation amplitudes which are higher than the values in the core. Since $(\rho_i/L_P)^2 > \rho_i/R$ is satisfied at the edge, we keep the electromagnetic perturbations up to second order, while we keep only the first order term in ρ_i/R.

As emphasized in previous work on nonlinear gyrokinetic equations in core transport barriers[28], a formulation in terms of the radial electric field, rather than in terms of mass flow, is preferred. Since a single particle's guiding center motion is determined by the electromagnetic field rather than the mass flow, this choice is not only natural, but also advantageous in separating the issue of determining the equilibrium ion distribution function (which is also an important issue in the tokamak edge by itself) from the formulation of the nonlinear gyrokinetic equation. We focus on the latter issue in this paper without specifying the equilibrium mass flow. Starting from the zeroth order phase-space Lagrangian of a charged particle, one can perform Lie perturbation analysis described in Refs.[29, 30, 28] to obtain the guiding-center phase-space Lagrangian, $\gamma_0 \equiv (e\mathbf{A} + M\mathbf{u}_E + Mv_\parallel \mathbf{b}) \cdot d\mathbf{R} + (\mu B/\Omega)d\theta - H_0 dt$. The notation here follows mostly that used in [28]. Noncanonical guiding-center coordinates which simplify the phase-space Lagrangian are used, $\mathbf{R} \equiv \mathbf{x} - \rho$, and $\mathbf{u}_E$ is associated with the zeroth order *slowly* *varying* potential Φ. $v_{||}$ is the guiding center parallel velocity which includes the Banos drift, and θ is the gyro-phase angle. Here, the guiding-center Hamiltonian up to ϵ_E^2 is $H_0 = e\Phi + \mu B + (M/2)(v_{||}^2 + u_E^2) + (\mu B/2\Omega)\mathbf{b}\cdot\nabla\times\mathbf{u}_E$, where $\mu\mathbf{b}\cdot\nabla\times\mathbf{u}_E$ describes the finite Larmor-orbit-average reduction of the equilibrium potential[30]. We note that unlike typical core profiles, the tokamak edge profiles satisfy $\rho_i/L_p > L_p/R$ so that $\epsilon_E^2 > \epsilon_B$. We also note that the trapped ion radial width modification due to the E_r shear[31] is on the order of unity for our ordering, based on typical tokamak H-mode edge plasma parameters. This can be easily shown from the fact that in general toroidal geometry, the banana orbit modification parameter[32] is given by $S \equiv 1 + \frac{m}{e}\frac{(RB_\phi)^2}{<B^2>}\frac{\partial}{\partial\psi}(\frac{E_r}{RB_\theta})$. On the other hand, the $\mathbf{E}\times\mathbf{B}$ shearing rate in general toroidal geometry[20] is given by $\omega_E = \frac{(RB_\theta)^2}{B}\frac{\partial}{\partial\psi}(\frac{E_r}{RB_\theta})$, for near isotropic ambient turbulence. It is straightforward to show that they are related through[33] $S \simeq 1 + (\frac{B}{B_\theta})^2\frac{\omega_E}{\Omega_i}$. Since $\omega_E/\Omega_i \sim \epsilon_E^2$, we have $|S-1| \sim 1$.

With the ordering for the electromagnetic fluctuations of edge turbulence, $\epsilon_\phi \equiv \delta n/n_0 \sim e\delta\phi/T_i \sim \delta B/B_0 << 1$, the electromagnetic fluctuations' first order contribution to the single particle phase-space Lagrangian, written in terms of the potentials ($\delta\phi(\mathbf{x},t)$, $\delta\mathbf{A}(\mathbf{x},t)$), is as follows:

$$\gamma_1 = e\delta\mathbf{A}(\mathbf{R}+\rho,t)\cdot(d\mathbf{R}+d\rho) - e\delta\phi(\mathbf{R}+\rho,t)dt \equiv -\delta H_1 dt, \tag{2}$$

where δH_1 is the first order guiding-center Hamiltonian.

Then, the Lie-perturbation analysis consists of finding near-identity transformations, order by order, which eliminate the gyro-phase dependence in Eq. (2) introduced by the fact that the fluctuating electromagnetic potentials are functions of the particle position $\mathbf{x} \equiv \mathbf{R} + \rho$, rather than functions of the guiding center position $\mathbf{R}$. Following a standard procedure[28], we find the first order gyro-averaged Hamiltonian $< \delta H_1 >= e < \delta\phi >$ $-e < (\mathbf{u}_E + \mathbf{v}_{Di} + v_{||}\mathbf{b} + \mathbf{c}_\perp)\cdot\delta\mathbf{A} >$, from which the first order nonlinear gyrokinetic Vlasov equation can be straightforwardly obtained. $\mathbf{c}_\perp$ is the gyration velocity. In the electromagnetic part, the first two terms, which are missing in conventional nonlinear gyrokinetic equations, appear as a consequence of our generalized ordering. The third term is related to the magnetic flutter transport, and the last term reduces to the more familiar form $\mu < \delta B_{||} >$ in the limit $k_\perp\rho_i << 1$.

Acknowledgments

The authors would like to thank K. Itoh, X. Garbet, R. Goldston, F. Hinton, S.-I. Itoh, Y. Kishimoto, L. Villard, M. Yagi, and F. Zonca for useful dicussions. This work was supported by the U.S. Department of Energy Contract No. DE–AC02–76–CHO-3073 (PPPL), DOE Cooperation Agreement No. DE-FC02-04ER54796 (UCI), Grant number FG03-88ER 53275 (UCSD), and the US DOE SciDAC Center for Gyrokinetic Particle Simulation of Turbulent Transport in Burning Plasmas.

References

[1] B.B. Kadomtsev, *Plasma Turbulence* (Academic Press, New York, 1965)

[2] P.H. Diamond and T.S. Hahm, Phys. Plasmas, **2**, 3640 (1995).

[3] K. Burrell, Phys. Plasmas, **4**, 1499 (1997); E. Synakowski *et al., ibid* **4**, 1736 (1997).

[4] S.-I. Itoh and K. Itoh, Plasma Phys. Control. Fusion **43**, 1055 (2000).
[5] T.S. Hahm, Plasma Phys. Control. Fusion **44**, A87 (2002).
[6] T.S. Hahm *et al.*, Plasma Phys. Control. Fusion **46**, A323 (2004).
[7] Z. Lin and T.S. Hahm, Phys. Plasmas **11**, 1099 (2004).
[8] B.B. Kadomtsev, Plasma Phys. Control. Fusion **34**, 1931 (1992).
[9] X. Garbet, L. Laurent, A. Samain *et al.,* Nuclear Fusion **34**, 963 (1994).
[10] Z. Lin, T.S. Hahm, W.W. Lee *et al.,* Science **281**, 1835 (1998).
[11] W.W. Lee, J. Comput. Phys. **72**, 243 (1987).
[12] A.M. Dimits *et al.,* Phys. Plasmas **7**, 969 (2000).
[13] Z. Lin, T.S. Hahm, W.W. Lee *et al.,* Phys. Rev. Lett. **83**, 3645 (1999).
[14] O. Gurcan *et al.*, submitted to Phys. Plasmas (2004).
[15] E.J. Kim, P.H. Diamond, M. Malkov *et al.,* Nuclear Fusion **43**, 961 (2003).
[16] F. Zonca, R.B. White, and L. Chen, Phys. Plasmas **11**, 2488 (2003).
[17] R. A. Fisher, Ann. Eugenics **7**, 353 (1937).
[18] A. Kolmogoroff *et al.*, Moscow Univ. Bull. Math. **1**, 1 (1937).
[19] H. Biglari, P.H. Diamond, and P.W. Terry, Phys. Fluids B **2**, 1 (1990).
[20] T.S. Hahm and K.H. Burrell, Phys. Plasmas **2**, 1648 (1995).
[21] T.S. Hahm, M.A. Beer, Z. Lin *et al.,* Phys. Plasmas **6**, 922 (1999).
[22] P.H. Diamond *et al.,* IAEA-CN-69/TH3/1 (IAEA, Vienna, 1998).
[23] L. Villard *et al.,* Nucl. Fusion **44**, 172 (2004).
[24] Y. Idomura *et al.,* Phys. Plasmas **7**, 3551 (2000).
[25] K. Itoh *et al.*, to be submitted to Plasma Phys. Control. Fusion (2004).
[26] W.X. Wang, F.L. Hinton, K. Wong, Phys. Rev. Lett. 87(2001) 055002-1.
[27] W.X. Wang *et al.,* in press for Computer Phys. Commun. (2004).
[28] T.S. Hahm, Phys. Plasmas **3**, 4658 (1996).
[29] R.G. Littlejohn, Phys. Fluids **24**, 1730 (1981).
[30] A. Brizard, Phys. Plasmas **2**, 459 (1995).
[31] R.D. Hazeltine, Phys. Fluids B **1**, 2031 (1989).
[32] F. L. Hinton and Y.-B. Kim, Phys. Plasmas **2**, 159 (1995).
[33] K.H. Burrell, Plasma Phys. Control. Fusion **40**, 1585 (1998).

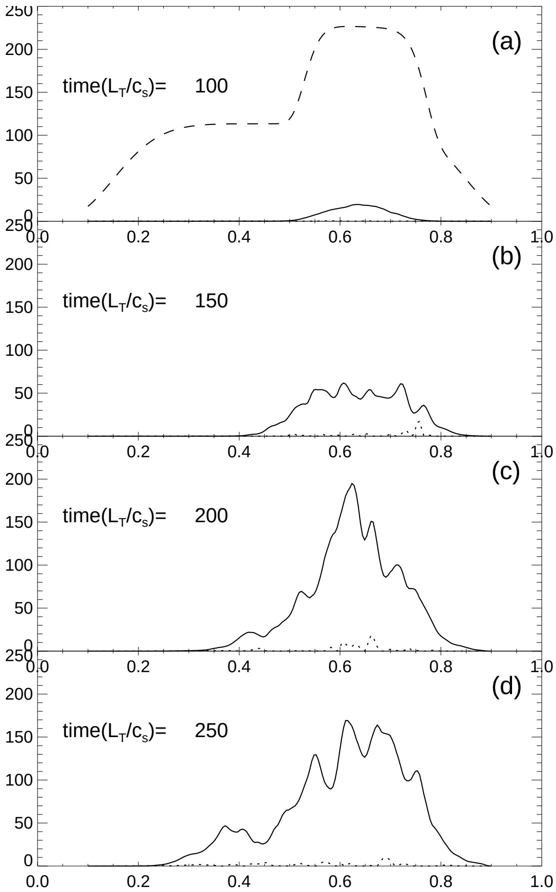

Figure 1: Spatio-temporal evolution of turbulence intensity from GTC simulation for $R/L_{Ti} = 6.9$ in core and 13.8 in edge.

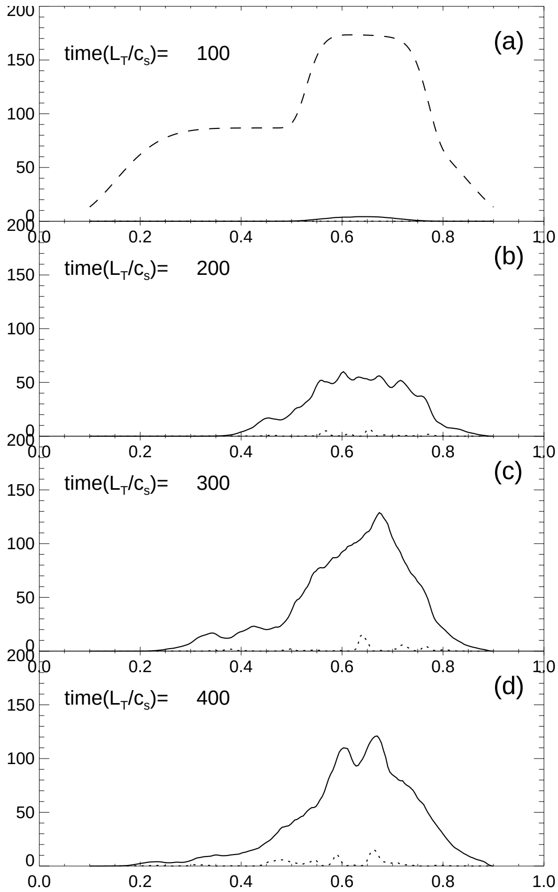

Figure 2: Spatio-temporal evolution of turbulence intensity from GTC simulation for $R/L_{Ti} = 5.3$ in core and 10.6 in edge.

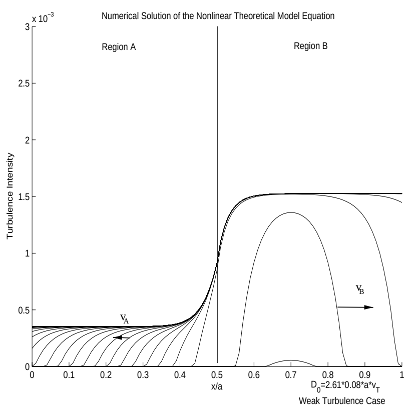

Figure 3: Spatio-temporal evolution of turbulence intensity from a numerical solution of Eq. (1) using parameters used for GTC simulation for Fig. 1.

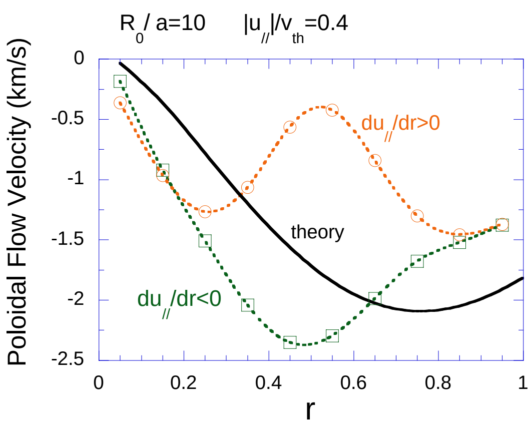

Figure 4: Poloidal flow of main ions from the GTC-Neo particle simulation (dotted line) is significantly different from a standard neoclassical theory prediction (solid line).